Journal of chemical & engineering data

Article

Cite This: J. Chem. Eng. Data 2018, 63, 2420−2429

pubs.acs.org/jced

Molecular Dynamics Simulation of First-Adsorbed Water Layer at Titanium Dioxide Surfaces

Guobing Zhou,[†] Chang Liu,[‡] and Liangliang Huang*[,†]

[†]School of Chemical, Biological and Materials Engineering, University of Oklahoma, Norman, Oklahoma 73019, United States

[‡]College of Chemical Engineering, Nanjing Tech University, Nanjing, Jiangsu 210009, China

Supporting Information

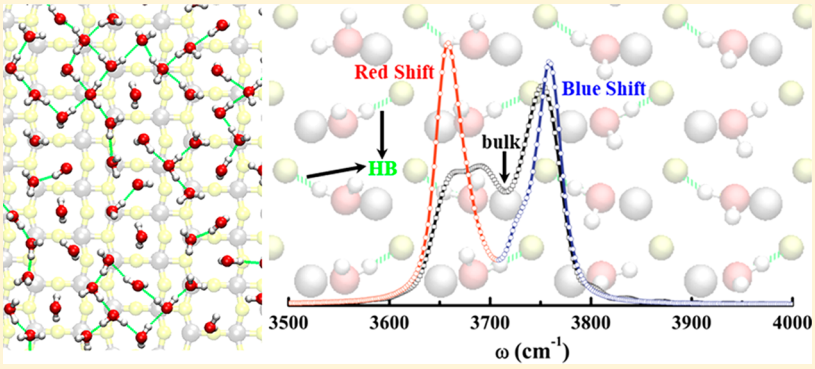

ABSTRACT: The behavior of the first-adsorbed water layer at titanium dioxide surfaces is critical to the fundamental understanding of titanium dioxide-based applications. Using classical MD simulations, we study the properties of first-adsorbed water layers at four TiO_2 surfaces, including the density profile, the angular orientation distribution, the HB structural and dynamic properties, and the vibrational spectra of water molecules in the first-adsorbed water layer. The calculation results reveal the characteristics of water. (a) Rutile (110) has O_w atoms of water that are located at the top sites of Ti_{5c}, and two H atoms are facing away from the surface. (b) Rutile (011) has water molecules that lean on the surface with one H atom directed toward the surface O_{2c} atoms and the other one pointing toward the bulk water. (c) TiO_2−B (100) has water that forms the "H-up" and "H-down" configurations. The "H-up" configuration has the O_w atoms atop the Ti_{5c} sites with two H atoms pointing toward the bulk water. The "H-down" configuration has both H atoms pointing toward the surface O_{2c} sites. (d) TiO_2−B (001) has water that has a random distribution; yet, the in-layer HBs promote the formation of small water clusters near the surface. The vibrational spectra, the HB network strength, and the HB lifetime are also analyzed in this work. A significant red shift of the vibrational spectra suggests an enhanced HB network, which also results in a much longer HB lifetime. For the studied surfaces, the TiO_2−B (100) has the most stable HB network, which is evidenced by the slowest decay of the HB lifetime.

INTRODUCTION

The behavior of molecules at titanium dioxide (TiO_2) surfaces is the key to successful applications, such as electronic devices, catalysis, energy, and biomedicine related fields.[1−5] For most applications at ambient conditions or in the liquid phase, the adsorbed water molecules at TiO_2 surfaces, as well as their structural and dynamics properties, require a fundamental understanding to achieve optimized processes and improved manufacturing. From the structural point of view, the topmost TiO_2 surface is composed of under-coordinated titanium (Ti) and oxygen (O) sites, which in turn interacts strongly with interfacial water molecules, and affects significantly the configuration, distribution, and other structural and dynamic properties of those water molecules at TiO_2 surfaces.[2,6−8] A number of experiments[9−14] and theoretical studies[6,7,15−20] have explored the interaction between water and TiO_2 surfaces. Among the reported properties, the hydrogen bond (HB) network, both the static network and the dynamic properties, is a sensitive probe to the water−TiO_2 interfacial interactions.[21−27]

On the other hand, despite the fundamental importance and the critical role of HB in catalytic reactions,[28,29] protein folding,[30,31] molecular self-assembly,[32,33] and proton transfer,[34] the direct measurement of interfacial HB remains as a challenge.[35,36] Previously, water adsorption on TiO_2 surfaces has been studied by scanning tunneling microscope (STM)[37] and infrared reflection−absorption spectroscopy (IRAS)[38] experiments. The adsorbed water molecules atop the five-coordinated titanium (Ti_{5c}) sites form a one-dimensional water chain via two types of HBs, namely, the weak HB between adjacent water molecules and the strong HB between water

Special Issue: Emerging Investigators

Received: November 12, 2017
Accepted: March 6, 2018
Published: March 14, 2018

DOI: 10.1021/acs.jced.7b00984
J. Chem. Eng. Data 2018, 63, 2420−2429

molecules and bridge-bonded two-coordinated (O_{2c}) sites. For the rutile (110) surface covered by two monolayer water, quasi-elastic neutron scattering (QENS) results showed that the first-adsorbed water layer (FAWL) is stabilized by HB interactions between the two water layers at the interface.[39] In addition, Goletto and co-workers[14] reported high-resolution in situ STM images of the rutile (110) surface exposed to bulk water. Their results revealed that there is an ordered superstructure of water molecules at the interface. The HB interaction between the FAWL and other water molecules is attributed to such an ordered structure, which is in accordance with the QENS experiments.[39] More recently, a phase-sensitive sum frequency generation (SFG) spectroscopy study reported that chem-isorbed and physisorbed water layers exist simultaneously at the irradiated anatase TiO_2 surfaces.[26] The spectroscopic data revealed that there is a strong HB interaction between the two water layers, which contributes to the superhydrophilic nature of anatase surfaces. It is worth noting that, to the best of our knowledge, no experimental study has been reported on dynamic properties of interfacial HB, which in turn are essential to understand the chemical and physical processes occurring at TiO_2 surfaces.

Molecular dynamics (MD) simulations, including ab initio MD (AIMD), reactive MD (RxMD), and nonreactive classical MD, can directly provide an electronic or atomistic level insight of the structural and dynamic properties of HB at the liquid−solid interfaces. For instance, comparing the FAWL at anatase (101) and rutile (110) surfaces, a higher HB was reported for the anatase (101) surface.[24] Further HB dynamics analysis demonstrated that the adsorbed water molecules of the anatase (101) surface exhibit a longer HB lifetime.[22] Moreover, a recent study[25] of water wetting on the rutile (110) surface illustrated that the HB lifetime for the second water layer is shorter than that of the first water layer. As a result, water molecules from the second layer escape from the HB network relatively easy and exchange with water molecules from other layers. It is also worth noting that for the HB structural and dynamic properties of water at the TiO_2 surface, classical force fields provide a satisfying description and can reproduce results from high level AIMD calculations.[6,7,12,17,19,22−25] In addition, it has been reported that the HB dynamics at the water−TiO_2 interface do not depend strongly on polarizable models of water and TiO_2 surfaces.[40]

In a previous work,[15] we examined the interactions between water and TiO_2 surfaces. The RxMD results demonstrated that water interacts strongly with the rutile (011), rutile (001), and TiO_2−B (100) surfaces, but weakly with the TiO_2−B (001) surface. Despite the density distribution analysis and the discussions on near-surface water dissociation, no result was reported for the HB properties. In this work, we perform a series of MD calculations to revisit the interfacial HB properties of water on the aforementioned four TiO_2 surfaces. Special attention has been paid to the structural and dynamic properties of HBs of the FAWL at surfaces. In particular, the correlation between the HB interactions and the vibrational spectra of water has been discussed in detail. The article is organized as follows. Section 2 presents a brief discussion of the simulation methods and the calculation setup. In the Results and Discussion Section, we have a discussion about the interfacial HB for water molecules at the surface, the relevant vibrational modes, and the relationship between them. Conclusions are summarized in the end.

2. SIMULATION METHODS AND DETAILS

2.1. Surface Models. In this work, four titanium dioxide surfaces are studied, namely rutile (110), rutile (011), TiO_2−B (100), and TiO_2−B (001). All surfaces were cleaved from bulk rutile with lattice parameters $a = b = 4.593$ Å and $c = 2.959$ Å (symmetry group $P42/MNM$) and bulk TiO_2(B) with lattice parameters $a = 12.164$ Å, $b = 3.735$ Å, and $c = 6.513$ Å (symmetry group $C2/M$). The surface structures were optimized and kept fixed during the simulation.[41,42] The flexible extended simple point charge (SPC/E) model[43] was used for water, in which the O−H bond and the H−O−H angle are described by harmonic potentials, bond constant, k_b, 1108.57 kcal/(mol·Å^2) and angle constant, k_θ, 91.54 kcal/(mol·rad^2). For each calculation setup, the surface was fully covered by a water film with a thickness of 2.0 nm. Periodic boundary conditions were applied in all three directions. The box dimension along the z-direction was fixed to be 10.0 nm, which contains the thickness of the surface, the water layer, and a vacuum to avoid the interactions between periodic images. The Lennard-Jones (LJ) 12−6 potential was used to describe the van der Waals (vdW) interactions of O_w−O_w and O_w−O (O_w and O correspond, respectively, to oxygen atoms of water and the TiO_2 surface). Meanwhile, the vdW interactions of Ti−O_w and Ti−O were described via the Buckingham potential defined as

$$E_{ij} = A_{ij} \times \exp\left(-\frac{r_{ij}}{\rho_{ij}}\right) - \frac{C_{ij}}{r_{ij}^6}$$

where r_{ij} is the distance between atoms i and j. The first term in the right side represents the repulsive interactions and the second term represents the attractive interactions. When it comes to the force field, the one adopted in this work is from the previous work by Bandura and Kubicki,[44] who have compared the optimized structures of liquid water at rutile (110) surface from both classical and ab initio DFT calculations. Their results demonstrated that the optimized structure of water molecules at the rutile (110) surface using the classical force field is in good agreement with the DFT-based results. Therefore, we think that the force-field parameters used here can provide reliable predictions to the water molecules on the TiO_2 surfaces. In addition, the Coulombic interactions between interaction sites are described by the Coulomb's law:

$$E_{ij} = \sum_{i=1}^{N_A} \sum_{j=1}^{N_B} \frac{q_i q_j}{4\pi\varepsilon_0 r_{ij}}$$

In which q_i and q_j are the charges for atoms i and j, and ε_0 is the dielectric constant. All LJ and Buckingham parameters and atomic charges used in this work are listed in Table S1 of the Supporting Information.

2.2. Simulation Details. All simulations were performed using a large-scale atomic/molecular massively parallel simulator (LAMMPS) software package.[45] The canonical ensemble was applied where the number of molecules (N), the volume (V), and the temperature (T) were fixed during the simulation. The temperature (300 K) was maintained by the Nose−Hoover method with a coupling coefficient of 0.1 ps. The initial velocities of the water molecules were assigned based on the Boltzmann distribution. The Newton's equation was integrated by the velocity Verlet algorithm with a time step

DOI: 10.1021/acs.jced.7b00984
J. Chem. Eng. Data 2018, 63, 2420−2429

of 1.0 fs. A cutoff of 1.0 nm was applied for the nonbonded interactions, while the long-range electrostatic interactions were calculated by the particle−particle particle−mesh (PPPM) method.[46] For each system, a calculation of 20.0 ns was performed, where the first 10.0 ns was for equilibrium, and the latter 10.0 ns was used for data analysis, in which the trajectory was analyzed every 100.0 fs. After the 20.0 ns simulation, two successive *NVT* simulations were also performed: one for the vibrational spectra analysis and the other one for the HB dynamic property calculation. For the vibrational spectra analysis, the simulation was performed for 200 ps with a smaller time step of 0.5 fs, and the velocity trajectory was updated every 0.5 fs. For the HB property calculation, we ran the simulation for 500 ps and collected the coordinate trajectory every 5 fs. Accordingly, two separate *NVT* simulations have been carried out for bulk water to obtain the corresponding vibrational spectra and hydrogen bond properties to be compared with those of the first-adsorbed water.

2.3. Vibrational Spectra Analysis. Vibrational spectroscopy is one of the most efficient and effective experimental approaches to probe the structural and dynamic properties of adsorbates at surfaces and interfaces, especially for systems involving hydrogen-bonded interactions.[47−50] This is mainly because the vibrational signals have a sensitive response to the change of local structure environments. For example, first-principle MD calculations[51] of water adsorption on the TiO_2 (110) surface revealed that the dissociative water adsorption at the Ti_{5c} sites results in the terminal and the bridging hydroxyl groups. The stretching frequency was observed for the terminal hydroxyls but not for the bridging ones. This is due to the fact that hydroxyl groups have broadening vibrational bands from the strong HB interactions. Kumar and co-workers[52] also reported a similar broadening phenomena in their AIMD calculations of adsorbed water at TiO_2 surfaces. They discussed that the strong HBs formed between the adsorbed water and the surface oxygen atoms can produce a noticeable broadening effect in the vibrational band. The dynamic properties of the adsorbed water on partially hydroxylated rutile (110) surface has been investigated by Born−Oppenheimer MD simulations.[53] The results showed that for the adsorbed water, the protons preferentially point to the bridging oxygen atoms, and the resulting stable HB network can lengthen the O−H bonds, leading to a significant red shift of the OH stretching frequency. In this work, we use the vibrational spectra analysis to understand the structure of the adsorbed water and the correlation between its configuration and the interfacial HB at the TiO_2 surfaces.

3. RESULTS AND DISCUSSION

3.1. Adsorbed Water Structure at TiO_2 Surfaces. To reveal the configuration of the adsorbed water at various TiO_2 surfaces, we first analyzed the water density distribution along the *z*-direction. The position of the oxygen atom of water (O_w) is used to represent the center of mass of the water molecules. For TiO_2 surfaces, the topmost layer is defined as the reference position, i.e., $z = 0.0$.

3.1.1. Rutile (110) Surface. As one of the most stable TiO_2 surfaces, rutile (110) has been extensively studied for the past few decades.[2,6−8,54] On this surface, there are four types of atoms that directly interact with water, namely Ti_{5c}, Ti_{6c}, O_{2c}, and O_{3c}, where the subscript denotes the coordination number. Each under-coordinated Ti_{5c} atom has a dangling bond perpendicular to the surface, making those Ti_{5c} active sites for water adsorption. On the other hand, the O_{2c} atoms are the outmost from the rutile (110) surface, and are potential sites to form HB with water molecules when they are moving closer to the surface. As illustrated in Figure 1, for water molecules on

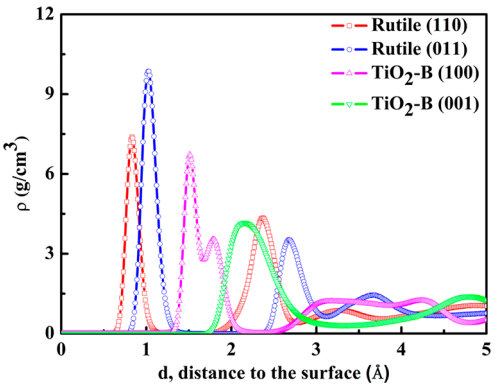

Figure 1. Density distribution of water molecules at different TiO_2 surfaces along the *z*-direction. The surfaces are placed at $d = 0.0$ Å.

the rutile (110) surface, there are two pronounced peaks, 0.83 and 2.37 Å away from the surface, corresponding to a density value of 7.39 and 4.34 g/cm^3, respectively. It is worth noting that the two densities are much larger than that of bulk water, 1.0 g/cm^3. Such high density near the surface implies that interfacial water molecules are packed differently from that of bulk water. The first peak at 0.83 Å is mainly contributed to the electrostatic interactions between the water molecules and the substrate. This is evidenced, as shown in Figure S5, that O_w atoms of water molecules locate atop the positively charged Ti_{5c} sites, with two H atoms pointing away from the surface. From Figure S5, it is also obvious that water molecules from the FAWL form a well-defined one-dimensional chain, which is also reported in previous studies of the water−rutile (110) system.[7,37,55−57] The second peak at 2.37 Å is from the water molecules that form HBs with the surface O_{2c} atoms and other water molecules.

3.1.2. Rutile (011) Surface. For the rutile (011) surface, previous studies have demonstrated that water can interact strongly with the surface.[2,6−8,54] At the interface, O_{2c} atoms reside at the apexes, and Ti_{5c} atoms are located at lower positions. Both of them are exposed to water molecules, which results in two distinct peaks at 1.03 and 2.68 Å with a density value of 9.86 and 3.53 g/cm^3, respectively. For the first peak here, it is primarily from the electrostatic and HB interactions between the FAWL and the surface. As shown in Figure S6, water molecules are distributed above the Ti_{5c} sites, which favors electrostatic interactions between O_w and Ti_{5c}. In addition, each water molecule of the FAWL has one H atom pointing toward one surface O_{2c} atom. It is worth noting that ab initio DFT calculations and STM experiments[58,59] reveal that at room temperature, water can dissociate on the rutile (011) surface. After the dissociation, the H atoms are bonded with the O_{2c} atoms and the hydroxyl groups are bonded with the Ti_{5c} atoms. Due to the use of the nonreactive force field, we did not observe any water dissociation, but the strong HB interaction between the water and surface O_{2c} atoms reveals a similar trend and agrees with the literatures. The second smaller peak at 2.68 Å is due to HB interactions of the water molecules from the adjacent layers.

DOI: 10.1021/acs.jced.7b00984
J. Chem. Eng. Data 2018, 63, 2420−2429

3.1.3. TiO_2–B (100) Surface. For the TiO_2–B (100) surface, previous calculations,[15,60,61] revealed that compared with rutile (110) and (011) surfaces, it has a modest interaction with water. On the surface, there are also four types of atoms directly interacting with the FAWL, namely Ti_{5c}, Ti_{6c}, O_{2c}, and O_{3c} sites. Similar to the distribution on the rutile (011) surface, the O_{2c} atoms are at the edges, and the Ti_{5c} sites are at lower positions. For the density distribution in Figure 1, there is one well-developed peak at 1.51 Å and one less pronounced adjacent peak at 1.79 Å. Such a result indicates that at the TiO_2–B (100) surface, there are two configurations for the water molecules of the FAWL. As illustrated in Figure S7, we denote the two configurations as "H-down" and "H-up", respectively. For the "H-up" configuration, H atoms point away from the surface, with O_w atoms at the top of the Ti_{5c} sites through electrostatic interactions. But for the "H-down" configuration, H atoms point to the surface, which facilitates the HB formation with the interface O_{2C} atoms. By comparing their relative distance to the surface, we conclude that the first peak is from the "H-up" water molecules, while the second peak is due to the "H-down" ones.

3.1.4. TiO_2–B (001) Surface. Lastly, for the TiO_2–B (001) surface, there are Ti_{5c}, O_{2c}, and O_{3c} sites at the interface, and our previous study observed a weak interaction of water at this surface.[15] The density profile of Figure 1 shows that there is only one distinct peak at 2.15 Å for the TiO_2–B (001) surface. Comparing the four studied surfaces, the peak from the TiO_2–B (001) surface is much lower and broader. The peak position is also the furthest from the surface. This suggests that water interacts weakly with the TiO_2–B (001) surface, and the FAWL is less ordered. As shown in Figures S5–7, water molecules on the other three surfaces form one- or two-dimensional structures, but the distribution of water molecules on the TiO_2–B (001) surface is random, see Figure S8. Nevertheless, as shown in Figure 2, because of the weak interaction between the water and the substrate, at the TiO_2–B (001) surface, water molecules of the FAWL can easily reorganize and form small clusters via HB interactions. In particular, the $C(2 \times 2)$ and $P(3 \times 2)$ patterns appear to be quite stable at the studied room temperature. Similar HB-assisted water clusters have been also reported on other metal oxide surfaces.[62]

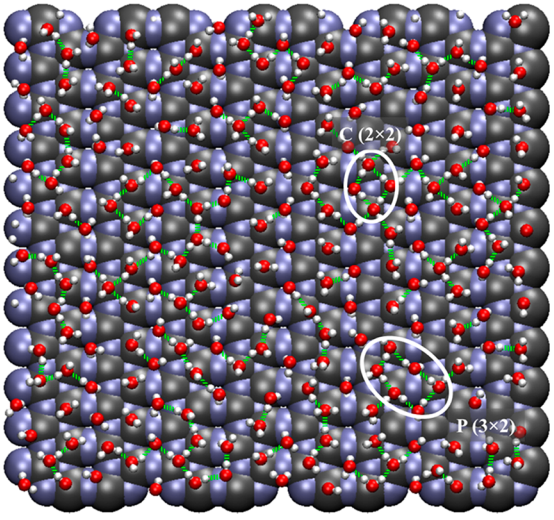

Figure 2. Top view of the FAWL on the TiO_2–B (001) surface at t = 20.0 ns. HB-assisted water clusters. The HBs are in green, while the Ti and O atoms are colored by gray and blue, respectively.

3.2. Orientation Analysis of Adsorbed Water. To further understand the structure details of adsorbed water molecules, we analyzed the orientational distributions of water molecules from the first density profile peak. As illustrated in the inset of Figure 3, the orientational angle θ is defined as the angle between the OH vector and the unit vector normal to the surface in the z-direction. For the FAWL on the rutile (110) surface, the orientation angle analysis in Figure 3 shows that there is only one sharp peak at about 55°, indicating that each water molecule in the FAWL has two H atoms pointing away from the surface, which confirms the simulation snapshot of Figure S5. While for the rutile (011) surface, two orientational angles were identified at 107 and 35°. This suggests that water molecules have one H atom pointing toward the surface and the other H atom pointing toward the bulk water, as also suggested by Figure S6. Such orientation facilitates the HB formation for both FAWL–surface and FAWL–other water molecules. Moreover, for water molecules at the TiO_2–B (100) surface, there are two pronounced peaks at 54 and 128°. Together with the snapshots in Figure S7, we can deduce that the two peaks correspond to the "H-up" and "H-down" configurations. When it comes to the TiO_2–B (001) surface, the orientation distribution is different. One broad peak around 90° was observed, which agrees with our previous RxMD results.[15] Such an orientation suggests that the O–H bonds are parallel to the TiO_2–B (001) surface, and the water molecules from the FAWL can form HBs easily with each other.

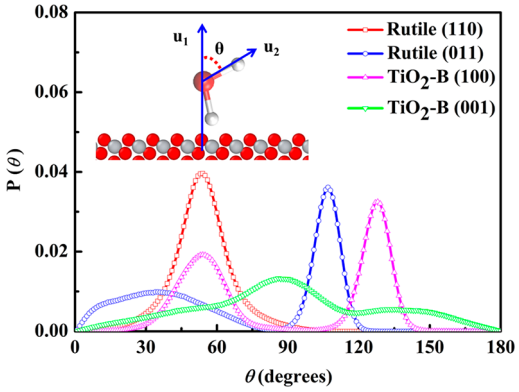

Figure 3. Angular distribution of the FAWL at TiO_2 surfaces. $\mathbf{u}_1$ is the unit vector normal to the surface. $\mathbf{u}_2$ is the vector pointing from the O atom to the H atom. θ is the angle defining the two vectors.

3.3. Vibrational Spectra Analysis of Adsorbed Water. Vibrational spectra analysis is a very useful tool to characterize the structures of water molecules at interfaces. It can be also calculated from MD simulations by employing the Fourier transformation of the velocity autocorrelation function (VACF). In this study, we calculated the vibrational spectra of water molecules from the FAWL at the four TiO_2 surfaces, to explore the correlation between the spectra information and the HB network of water. The normalization of VACF is defined by[63,64]

$$C_v(t) = \frac{\langle \vec{v}_i(0)\vec{v}_i(t)\rangle}{\langle \vec{v}_i(0)\vec{v}_i(0)\rangle}$$

where $\vec{v}_i(t)$ represents the velocity of an atom of type i (H or O_w atoms) in the defined interfacial region at time t. The

DOI: 10.1021/acs.jced.7b00984
J. Chem. Eng. Data 2018, 63, 2420–2429

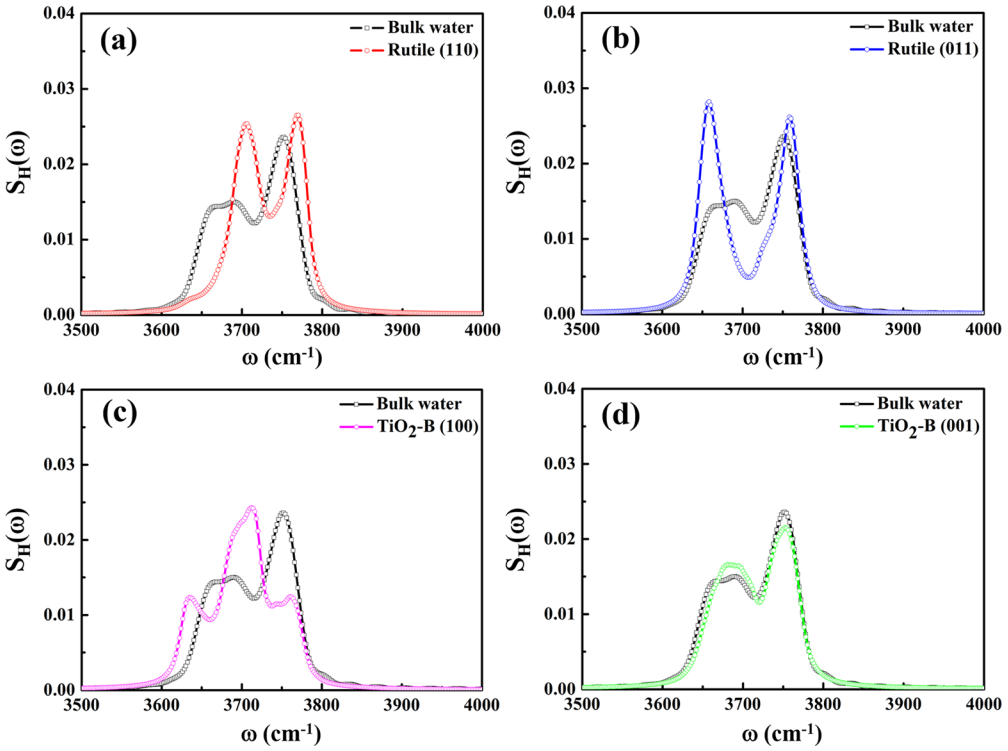

Figure 4. Fourier transformation vibrational spectra analysis of the hydrogen atoms of FAWL at the (a) rutile (110), (b) rutile (011), (c) TiO_2−B (100), and (d) TiO_2−B (001) surfaces. For comparison, the result from pure water is also shown.

angular brackets denote the ensemble average, which is evaluated at different initial reference times. The vibrational density of states (VDOS) can be calculated from the Fourier cosine transformation of VACF:[64,65]

$$S(\omega) = \int_0^\alpha C_v(t)\cos(\omega t)dt$$

In this work, we mainly focus on the stretching mode of O−H bonds in the high-frequency region. For the water molecules at the TiO_2 surface, such as, the water−rutile (110) system, the results in Figure S13 illustrate that the intensity of $S(\omega)$ for H atoms is much higher than that of O atoms, suggesting that the dominant contribution to the O−H stretching vibration results from the $S(\omega)$ of H atoms. Therefore, here the normalized VACF is calculated only for the H atoms in the FAWL, so the calculated VDOS contains only the characteristic peaks of H atoms.

3.3.1. Rutile (110) Surface. As shown in Figure 4, the peaks around 3690 and 3750 cm^{-1} are characteristic of the stretching mode of the O−H bonds in bulk water, which agrees with the experiments and other calculations.[44] For the interfacial water, the results show that there are two characteristic peaks for the O−H bond stretching mode of the FAWL at the rutile (110), rutile (011), and TiO_2−B (001) surfaces but not the at the TiO_2−B (100) surface, where three characteristic peaks were identified in the same region for the interfacial water. In detail, Figure 4a shows that the peaks for OH vibration modes at the rutile (110) surface are located around 3700 and 3770 cm^{-1}. Compared with the bulk water vibration modes, there is a blue shift of 10 and 20 cm^{-1}, respectively. It is worth noting that similar results have been observed by Xantheas and Dunning[66] and their DFT calculations demonstrated that the vibrational modes of the hydrogen-bonded O−H bonds in the water dimer have a characteristic peak at 3712 cm^{-1} (aug-cc-pVDZ) or 3748 cm^{-1} (aug-cc-pVTZ), quite close to the experimental value of 3718 cm^{-1}.[67] We performed an analysis to use the HB assignment to do the vibrational analysis based on the type of HB that involves the H atoms. That is, the assignment for the O−H bonds at the rutile (110) surface should be the donor bridge H stretch according to the normal modes definition stated in previous studies.[66] The results (3690 and 3750 cm^{-1}) here agree well with those reference values. While for the same water−rutile (110) system, experimental inelastic neutron scattering (INS) spectra results show that the OH vibration modes have two peaks at 412 (3322 cm^{-1}) and 416 meV (3354 cm^{-1}).[68,69] The difference between the experimental values and the calculation results is probably from the different temperatures. In this work, the MD simulations are performed at 300 K, while the temperature of the INS spectra experiments is at 4 K. As for the calculated frequency values, when one compares the calculation with the experiments, it is important to consider the following factors. (a) The temperature: For example, the ab initio MD (AIMD) simulations by Mattioli et al.[17] They performed AIMD calculations to investigate the structural and vibrational properties of a water bilayer adsorbed on the anatase (101) surface at different temperatures. Their calculated results demonstrated that at 50 K, the stretching mode of the O−H bonds of water has three distinguishable vibrational frequencies at 2530, 2970, and 3290 cm^{-1}. On the other hand, when the temperature is 300 K, the spectra show an unresolved broad band at around 3400 cm^{-1} for the O−H stretching modes. Such an observation demonstrates that the increase in the temperature will result in a higher O−H vibrational frequency. (b) The nature of the surface: One other factor that affects the vibrational spectra is the structural and chemical properties of the pristine surface. As discussed, the four studied TiO_2 surfaces have their unique configurations. The anatase (101) surface is different from the rutile (110) surface, which results in different

DOI: 10.1021/acs.jced.7b00984
J. Chem. Eng. Data 2018, 63, 2420−2429

Table 1. Average Number of HBs of the FAWL with (A) Substrate, (B) FAWL, and (C) Other Water[a]

surfaces	HB with substrate (A)	HB within FAWL (B)	HB with other water (C)	total HBs (A + B + C)
rutile (110)	0.07	0.02	1.62	1.71
rutile (011)	1.00	0.12	0.61	1.73
TiO_2–B (100)	1.00	0.10	1.70	2.80
TiO_2–B (001)	0.45	1.82	0.89	3.17
bulk water			3.58	

[a]The calculated HB number for bulk water is 3.58.

interactions with near surface water molecules. Therefore, the vibrational spectra of water on the two surfaces shall be different from each other. (c) The computational model and force fields: Kavathekar and co-workers[70] applied a flexible simple point charge (SPC) water model and calculated the vibrational spectra of water at different TiO_2 surfaces. They found that the O−H vibration modes at the rutile (110) surface have a broad band at 3453 cm^{-1}. While for other TiO_2 surfaces, the corresponding modes generally have two characteristic peaks, rutile (101): 3571 and 3663 cm^{-1}; rutile (001): 3538 and 3656 cm^{-1}; anatase (101): 3600 and 3669 cm^{-1}; and anatase (001): 3584 and 3674 cm^{-1}. Considering the results from our flexible SPC/E model, it is obvious that the choice of the computational model and force field can influence the calculated vibrational spectra results. It is also worth noting that calculated vibrational frequencies are typically larger than those from experiments.[71] Very often, a scaling factor is applied to account for the offset when one directly compares the vibrational spectra between simulation and experiment.[72−77]

3.3.2. Rutile (011), TiO_2–B (100), and TiO_2–B (001) Surfaces. For the FAWL at the rutile (011) surface, the result in Figure 4b demonstrates that the O−H bonds have two peaks at about 3660 and 3760 cm^{-1}. Compared with bulk water, the two modes have a red shift of 30 cm^{-1} and a blue shift of 10 cm^{-1}, respectively. When it comes to the TiO_2–B (100) surface, two peaks around 3635 and 3710 cm^{-1} are the characteristic O−H vibration modes, displaying significant red shifts of 55 and 40 cm^{-1}, respectively. It is worth noting that the splitting peak at 3760 cm^{-1} is from the dangling O−H bonds of water. Lastly, for the FAWL at the TiO_2–B (001) surface, the O−H bond vibration modes are close to that of bulk water, except for a small red shift around the 3680 cm^{-1} mode.

3.4. Hydrogen Bond Network of Adsorbed Water. It has been reported that the vibrational spectra modes of water are correlated with the HB network and its dynamic properties.[64,78−80] In this work, the HB of water from the FAWL is calculated based on the geometry criteria:[81,82]

$$R^{OO} < R_c^{OO} \text{ and } \theta^{OOH} < \theta_c^{OOH}$$

where R^{OO} is the distance between two O atoms, one of which serves as the HB acceptor and the other one is regarded as the HB donor, while θ^{OOH} represents the angle O···O−H. Similarly, R_c^{OO} and θ_c^{OOH} correspond the upper limit distance and the angle for the HB formation, respectively. The two thresholds are 3.5 Å and 30°, respectively.[82]

3.4.1. Rutile (110) Surface. For water molecules from the FAWL, they can form HBs from three groups of acceptor−donor: (A) FAWL-substrate, (B) FAWL−FAWL, and (C) FAWL−other water. The calculated average HB number for each type is listed in Table 1. For example, the results show that for the FAWL at the rutile (110) surface, the average HB number is negligible for type A (0.07) and type B (0.02), but it is 1.62 for type C. The percentage analysis in Figure 5 shows

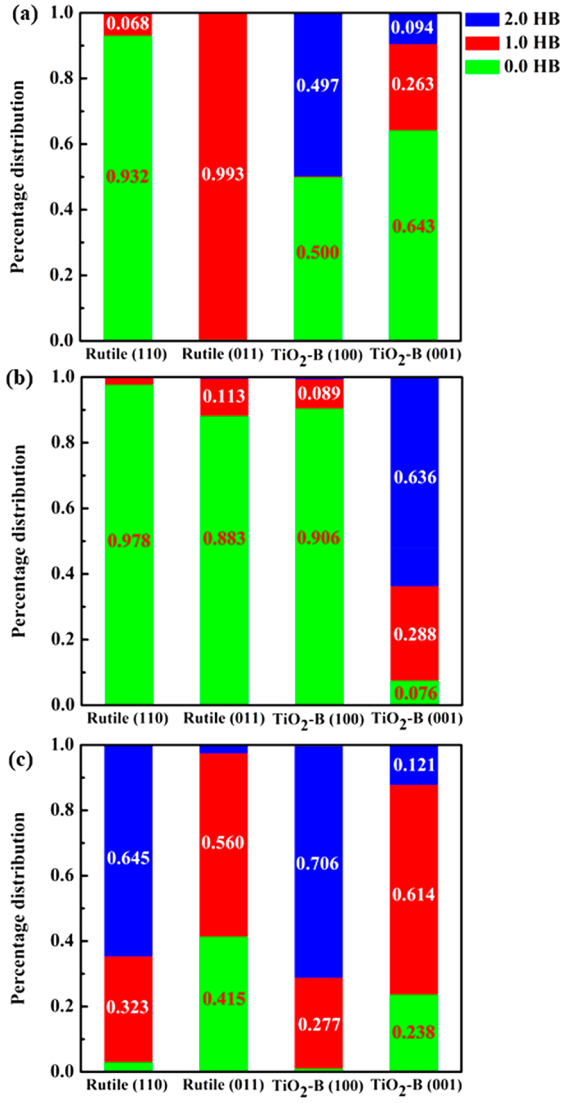

Figure 5. Analysis of averaged HBs between: (a) FAWL−substrate; (b) FAWL−FAWL; and (c) FAWL−other water. Note that in the system of TiO_2–B (001), the percentage of more than 2.0 HB is included in the percentage of 2.0 HB for clarity.

that for the FAWL at the rutile (110) surface, less than 7% of the water molecules can form HBs with the substrate. Meanwhile, only about 2% of the water molecules from the FAWL can form HBs with each other. For the type C HB, around 32 and 64% of the water molecules in the FAWL can form 1.0 HB or 2.0 HBs with other water molecules beyond the FAWL, which returns an averaged number of 1.62 for type C HB.

3.4.2. Rutile (011) Surface. For the average HB number at the rutile (011) surface, the results in Table 1 show that the

DOI: 10.1021/acs.jced.7b00984
J. Chem. Eng. Data 2018, 63, 2420−2429

values for type A, B, and C HB are 1.0, 0.12, and 0.61, respectively. Together with the distribution analysis in Figure 5, nearly all water molecules from the FAWL form 1.0 HB with the substrate surface. This result confirms the aforementioned water structure analysis, that is, each water molecule has one H atom pointing to the surface O_{2c} atoms, and the other H atoms are located away from the substrate. Furthermore, about 88% of water molecules from the FAWL do not form any HB interaction with each other, and about 11.3% of water molecules form 1.0 HB within the layer. For water molecules from different layers, about 41.5% of water molecules from the FAWL cannot form any HB with other water molecules, and the other 56.0% of water molecules form 1.0 HB with water molecules from outside of the FAWL.

3.4.3. TiO_2−B (100) Surface. For the average HB number on the TiO_2−B (100) surface, it is 1.0 and 0.10 for type A and type B, respectively, which is similar to the result of the rutile (011) surface. As plotted in Figure 5a, for the FAWL at the TiO_2−B (100) surface, 50% of water molecules cannot form HB with the substrate, but all of the other 50% of molecules form 2.0 HB with the surface O_{2c} atoms. Therefore, the averaged HB value for type A is 1.0. Together with the aforementioned configuration analysis, we conclude that the "H-up" water molecules do not form any HB with the surface, but the "H-down" water molecules can form exactly two HBs with the O_{2c} atoms of the surface. In addition, according to Figure 5b, we can see that over 90% of the water molecules of the FAWL cannot form any HB with each other, resulting in a negligible HB value for type B. For the HB between the FAWL and other water molecules, the results in Figure 5c show that 27.7% of the water molecules of the FAWL can form 1.0 HB, while the other ∼70.0% will form 2.0 HBs. This suggests that over 27% of water molecules with the "H-up" configuration have dangling O−H bonds, resulting in the O−H vibration modes with a higher frequency around 3760 cm^{-1}.

3.4.4. TiO_2−B (001) Surface. Finally, for water at the TiO_2−B (001) surface, the average HBs are 0.45, 1.82, and 0.89 for type A, B, and C, respectively. This indicates that each water molecule has 3.17 HBs by average. This averaged HB is close to that of bulk water and is much higher than what are observed at other three surfaces. In particular, while the other three surfaces show a negligible type B HB, for the TiO_2−B (001) surface, the averaged type B HB is 1.82. Such a large value also explains the formation of HB clusters at the surface. To summarize, the dominating HBs are type C for the rutile (110) surface, type A and C for both the rutile (011) and TiO_2−B (100) surfaces, and type B and C for the TiO_2−B (001) surface.

3.5. Hydrogen Bond Dynamics of Adsorbed Water. The HB strength is also calculated by the continuous time correlation functions (TCFs), $S_{HB}(t)$, defined as[81,83,84]

$$S_{HB}(t) = \frac{\langle h(0)h(t)\rangle}{\langle h(t)\rangle}$$

where the population variable of $h(t)$ is a unity when a tagged HB pair is maintained for the time period from 0 to t, otherwise zero. Figure 6 shows the calculated $S_{HB}(t)$ variations for types A and C HBs, with the result for type B of the TiO_2−B (001) shown as the inset in Figure 6a. For the type C HBs of the rutile (110) surface, the $S_{HB}(t)$ curve decays slightly faster than that of bulk water, indicating a relatively weaker HB strength. This agrees with the blue shift of the OH stretching modes shown in Figure 4a. For the type A HB of the rutile (011) surface, as illustrated in Figure 6a, the $S_{HB}(t)$ curve decay is significantly slower than that of bulk water, suggesting a stronger and more stable HB network. Regarding the type C HB of the rutile (011) surface, the $S_{HB}(t)$ curve decays quickly, suggesting a weak interaction between the FAWL and other water molecules. It is also worth noting that for the red and blue shifts of the O−H stretching modes at the rutile (011) surface illustrated in Figure 4b, the former is from the enhanced interaction of type A HB, and the latter is due to the decreased strength of type C HBs.

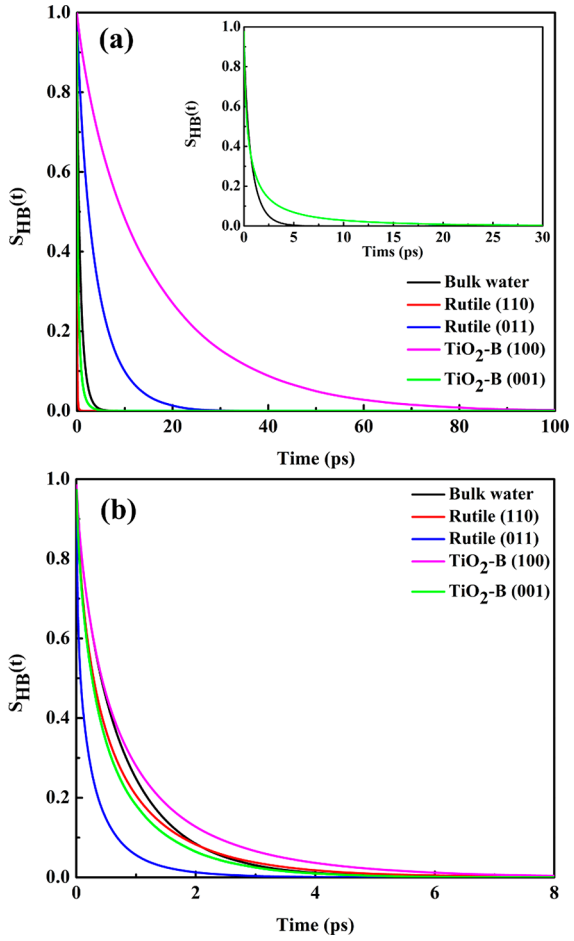

Figure 6. Continuous time correlation function, $S_{HB}(t)$, for the HB network between (a) FAWL−substrate and (b) FAWL−other water on different TiO_2 surfaces. The inset in (a) is the $S_{HB}(t)$ for the HB network between FAWL−FAWL on the TiO_2−B (001) surface. For comparison, the result from bulk water is also shown.

Similarly, for type A and C HBs of the TiO_2−B (100) surface, the $S_{HB}(t)$ decays slower than that of the bulk water, which further confirms that both types A and C HB strengths are enhanced. This enhanced HB strength results in the red shift of the OH stretching modes as shown in Figure 4c. Additionally, for the type C HB on the TiO_2−B (001) surface, the $S_{HB}(t)$ curve decays faster than that of the bulk water, demonstrating a slight strength decrease of the type C HBs. For the type B HB on this surface, the $S_{HB}(t)$ curve, as shown in the inset of Figure 6a, decays significantly slower with respect to that of the bulk water, suggesting a greatly enhanced strength of the type B HBs. Overall, the HB strength for the FAWL on the TiO_2−B (001) surface is enhanced, and this is why a red shift of the OH stretching modes is observed, see Figure 4d.

DOI: 10.1021/acs.jced.7b00984
J. Chem. Eng. Data 2018, 63, 2420−2429

4. CONCLUSIONS

In this work, classical MD simulations have been carried out to systematically investigate the properties of FAWL at four TiO_2 surfaces. The water density profile, water angular orientation distribution, the HB structural and dynamic properties, and the vibrational spectra have been calculated and discussed. Our calculation results show that different water structures can be formed near the TiO_2 surfaces. (a) Rutile (110) has O_w atoms atop the Ti_{5c} sites and two H atoms facing away from the surface. (b) Rutile (011) has water molecules leaning on the surface with one H atom directed toward the surface O_{2c} atoms, and the other one pointing toward the bulk water. (c) TiO_2−B (100) has water that forms two configurations, "H-up" and "H-down". The "H-up" configuration has the O_w atoms atop the Ti_{5c} sites with two H atoms pointing toward the bulk water. The "H-down" configuration has both H atoms pointed toward the surface O_{2c} sites. (d) TiO_2−B (001) has water that has a random distribution; yet, the in-layer HBs promote the formation of small water clusters near the surface.

Based on the structural and orientational information on the FAWL, the vibrational spectra, the HB network, and the lifetime are also analyzed. Both blue and red shifts of OH vibration modes have been observed for the rutile (011) surface. The blue and red shifts have been identified for the rutile (110) and TiO_2−B (100) surfaces, respectively. The slightly red shift from the TiO_2−B (001) surface is probably due to the HB assisted clusters formed in the FAWL. The HBs are classified as three types: type A, the ones from the FAWL−substrate interaction; type B, the ones from the FAWL−FAWL interactions; type C, the ones from the FAWL−other water interactions. The calculations reveal the dominating HBs for the studied TiO_2 surfaces: rutile (110), type C; rutile (011), type A and C; TiO_2−B (100), type A and C; and TiO_2−B (001), type B and C. The vibrational spectra, the HB network strength, and the HB lifetime are correlated; a significant red shift of the vibrational spectra suggests an enhanced HB network, which also results in a much longer HB lifetime. For the studied surfaces, the TiO_2−B (100) has the most stable HB network, and the HB lifetime is also the longest. The relationship between the vibrational spectra and interfacial structures and dynamics provides a new perspective of using vibrational spectra experiments to qualitatively characterize the HB properties at the water−TiO_2 interface.

■ ASSOCIATED CONTENT

Supporting Information

The Supporting Information is available free of charge on the ACS Publications website at DOI: 10.1021/acs.jced.7b00984.

LJ and Buckingham parameters and atomistic charges used in this work; model details for water−TiO_2 systems; initial configurations for four water−TiO_2 systems; snapshots for FAWL on four TiO_2 surfaces; top view of hydrogen-bonded water clusters in FAWL on the TiO_2−B (001) surface; brief description about the density profiles; and vibrational spectra of $S_O(\omega)$ and $S_H(\omega)$ of FAWL (PDF)

■ AUTHOR INFORMATION

Corresponding Author

*hll@ou.edu.

ORCID

Liangliang Huang: 0000-0003-2358-9375

Funding

G.B.Z. and L.L.H. acknowledge the U.S. National Science Foundation (NSF) for support through Grant CHE-1710102. L.L.H. also acknowledges partial support from National Natural Science Foundation of China (21676232). L.C. acknowledges the support from National Natural Science Foundation of China (21476106).

Notes

The authors declare no competing financial interest.

■ ACKNOWLEDGMENTS

We are very pleased to thank the OU Supercomputing Center for Education & Research (OSCER) at the University of Oklahoma (OU) for support.

■ REFERENCES

(1) Bai, J.; Zhou, B. X. Titanium Dioxide Nanomaterials for Sensor Applications. *Chem. Rev.* **2014**, *114*, 10131−10176.

(2) Bourikas, K.; Kordulis, C.; Lycourghiotis, A. Titanium Dioxide (Anatase and Rutile): Surface Chemistry, Liquid-Solid Interface Chemistry, and Scientific Synthesis of Supported Catalysts. *Chem. Rev.* **2014**, *114*, 9754−9823.

(3) Kapilashrami, M.; Zhang, Y. F.; Liu, Y. S.; Hagfeldt, A.; Guo, J. Probing the Optical Property and Electronic Structure of TiO_2 Nanomaterials for Renewable Energy Applications. *Chem. Rev.* **2014**, *114*, 9662−9707.

(4) Rajh, T.; Dimitrijevic, N. M.; Bissonnette, M.; Koritarov, T.; Konda, V. Titanium Dioxide in the Service of the Biomedical Revolution. *Chem. Rev.* **2014**, *114*, 10177−10216.

(5) Fujishima, A.; Honda, K. Electrochemical Photolysis of Water at a Semiconductor Electrode. *Nature* **1972**, *238*, 37−38.

(6) Sun, C.; Liu, L. M.; Selloni, A.; Lu, G. Q.; Smith, S. C. Titania-Water Interactions: A Review of Theoretical Studies. *J. Mater. Chem.* **2010**, *20*, 10319−10334.

(7) Mu, R.; Zhao, Z. J.; Dohnalek, Z.; Gong, J. Structural Motifs of Water on Metal Oxide Surfaces. *Chem. Soc. Rev.* **2017**, *46*, 1785−1806.

(8) De Angelis, F.; Di Valentin, C.; Fantacci, S.; Vittadini, A.; Selloni, A. Theoretical Studies on Anatase and Less Common TiO_2 Phases: Bulk, Surfaces, and Nanomaterials. *Chem. Rev.* **2014**, *114*, 9708−9753.

(9) Hugenschmidt, M. B.; Gamble, L.; Campbell, C. T. The Interaction of H_2O with a TiO_2 (110) Surface. *Surf. Sci.* **1994**, *302*, 329−340.

(10) Wang, Z. T.; Wang, Y. G.; Mu, R.; Yoon, Y.; Dahal, A.; Schenter, G. K.; Glezakou, V. A.; Rousseau, R.; Lyubinetsky, I.; Dohnalek, Z. Probing Equilibrium of Molecular and Deprotonated Water on TiO_2(110). *Proc. Natl. Acad. Sci. U. S. A.* **2017**, *114*, 1801−1805.

(11) Geng, Z.; Chen, X.; Yang, W.; Guo, Q.; Xu, C.; Dai, D.; Yang, X. Highly Efficient Water Dissociation on Anatase TiO_2(101). *J. Phys. Chem. C* **2016**, *120*, 26807−26813.

(12) Matthiesen, J.; Hansen, J. O.; Wendt, S.; Lira, E.; Schaub, R.; Laegsgaard, E.; Besenbacher, F.; Hammer, B. Formation and Diffusion of Water Dimers on Rutile TiO_2(110). *Phys. Rev. Lett.* **2009**, *102*, 226101.

(13) Hussain, H.; Tocci, G.; Woolcot, T.; Torrelles, X.; Pang, C. L.; Humphrey, D. S.; Yim, C. M.; Grinter, D. C.; Cabailh, G.; Bikondoa, O.; Lindsay, R.; Zegenhagen, J.; Michaelides, A.; Thornton, G. Structure of a Model TiO_2 Photocatalytic Interface. *Nat. Mater.* **2017**, *16*, 461−466.

(14) Serrano, G.; Bonanni, B.; Di Giovannantonio, M.; Kosmala, T.; Schmid, M.; Diebold, U.; Di Carlo, A.; Cheng, J.; VandeVondele, J.; Wandelt, K.; Goletti, C. Molecular Ordering at the Interface Between Liquid Water and Rutile TiO_2(110). *Adv. Mater. Interfaces* **2015**, *2*, 1500246.

DOI: 10.1021/acs.jced.7b00984
J. Chem. Eng. Data 2018, 63, 2420−2429

(15) Huang, L. L.; Gubbins, K. E.; Li, L. C.; Lu, X. H. Water on Titanium Dioxide Surface: A Revisiting by Reactive Molecular Dynamics Simulations. *Langmuir* **2014**, *30*, 14832−14840.
(16) Zhao, Z.; Li, Z.; Zou, Z. Structure and Properties of Water on the Anatase TiO_2(101) Surface: From Single-Molecule Adsorption to Interface Formation. *J. Phys. Chem. C* **2012**, *116*, 11054−11061.
(17) Mattioli, G.; Filippone, F.; Caminiti, R.; Bonapasta, A. A. Short Hydrogen Bonds at the Water-TiO_2 (Anatase) Interface. *J. Phys. Chem. C* **2008**, *112*, 13579−13586.
(18) Skelton, A. A.; Walsh, T. R. Interaction of Liquid Water with the Rutile TiO_2(110) Surface. *Mol. Simul.* **2007**, *33*, 379−389.
(19) Kavathekar, R. S.; Dev, P.; English, N. J.; MacElroy, J. M. D. Molecular Dynamics Study of Water in Contact with the TiO_2 rutile-110, 100, 101, 001 and anatase-101, 001 surface. *Mol. Phys.* **2011**, *109*, 1649−1656.
(20) Hammer, B.; Wendt, S.; Besenbacher, F. Water Adsorption on TiO_2. *Top. Catal.* **2010**, *53*, 423−430.
(21) Sebbari, K.; Domain, C.; Roques, J.; Perron, H.; Simoni, E.; Catalette, H. Investigation of Hydrogen Bonds and Temperature Effects on the Water Monolayer Adsorption on Rutile TiO_2 (110) by First-Principles Molecular Dynamics Simulations. *Surf. Sci.* **2011**, *605*, 1275−1280.
(22) English, N. J.; Kavathekar, R. S.; MacElroy, J. M. D. Hydrogen Bond Dynamical Properties of Adsorbed Liquid Water Monolayers with Various TiO_2 Interfaces. *Mol. Phys.* **2012**, *110*, 2919−2925.
(23) Bahramian, A. Molecular Interactions Insights underlying Temperature-Dependent Structure of Water Molecules on TiO_2 Nanostructured Film: A Computational Study using Reactive and Non-reactive Force Fields. *Fluid Phase Equilib.* **2017**, *438*, 53−66.
(24) Kavathekar, R. S.; English, N. J.; MacElroy, J. M. D. Spatial Distribution of Adsorbed Water Layers at the TiO_2 Rutile and Anatase Interfaces. *Chem. Phys. Lett.* **2012**, *554*, 102−106.
(25) Hamideh Babazadeh, K.; Foroutan, M. Water Distribution in Layers of an Aqueous Film on the Titanium Dioxide Surface: A Molecular Dynamic Simulation Approach. *J. Mol. Liq.* **2017**, *244*, 291−300.
(26) Hosseinpour, S.; Tang, F.; Wang, F.; Livingstone, R. A.; Schlegel, S. J.; Ohto, T.; Bonn, M.; Nagata, Y.; Backus, E. H. G. Chemisorbed and Physisorbed Water at the TiO_2/Water Interface. *J. Phys. Chem. Lett.* **2017**, *8*, 2195−2199.
(27) Yang, W.; Wei, D.; Jin, X.; Xu, C.; Geng, Z.; Guo, Q.; Ma, Z.; Dai, D.; Fan, H.; Yang, X. Effect of the Hydrogen Bond in Photoinduced Water Dissociation: A Double-Edged Sword. *J. Phys. Chem. Lett.* **2016**, *7*, 603−608.
(28) Fersht, A. R.; Shi, J. P.; Knill-Jones, J.; Lowe, D. M.; Wilkinson, A. J.; Blow, D. M.; Brick, P.; Carter, P.; Waye, M. M. Y.; Winter, G. Hydrogen Bonding and Biological Specificity Analysed by Protein Engineering. *Nature* **1985**, *314*, 235−238.
(29) Shan, S.; Loh, S.; Herschlag, D. The Energetics of Hydrogen Bonds in Model Systems: Implications for Enzymatic Catalysis. *Science* **1996**, *272*, 97−101.
(30) Briggs, M. S.; Roder, H. Early Hydrogen-Bonding Events in the Folding Reaction of Ubiquitin. *Proc. Natl. Acad. Sci. U. S. A.* **1992**, *89*, 2017−2021.
(31) Kim, P. S.; Baldwin, R. L. Intermediates in the Folding Reactions of Small Proteins. *Annu. Rev. Biochem.* **1990**, *59*, 631−650.
(32) Liu, Y.; Hu, C.; Comotti, A.; Ward, M. D. Supramolecular Archimedean Cages Assembled with 72 Hydrogen Bonds. *Science* **2011**, *333*, 436−440.
(33) MacGillivray, L. R.; Atwood, J. L. A Chiral Spherical Molecular Assembly Held Together by 60 Hydrogen Bonds. *Nature* **1997**, *389*, 469−472.
(34) Tuckerman, M. E.; Marx, D.; Klein, M. L.; Parrinello, M. On the Quantum Nature of the Shared Proton in Hydrogen Bonds. *Science* **1997**, *275*, 817−820.
(35) Muller-Dethlefs, K.; Hobza, P. Noncovalent Interactions: A Challenge for Experiment and Theory. *Chem. Rev.* **2000**, *100*, 143−167.
(36) Steiner, T. The Hydrogen Bond in the Solid State. *Angew. Chem., Int. Ed.* **2002**, *41*, 48−76.
(37) Lee, J.; Sorescu, D. C.; Deng, X.; Jordan, K. D. Water Chain Formation on TiO_2(110). *J. Phys. Chem. Lett.* **2013**, *4*, 53−57.
(38) Kimmel, G. A.; Baer, M.; Petrik, N. G.; VandeVondele, J.; Rousseau, R.; Mundy, C. J. Polarization- and Azimuth-Resolved Infrared Spectroscopy of Water on TiO_2(110): Anisotropy and the Hydrogen-Bonding Network. *J. Phys. Chem. Lett.* **2012**, *3*, 778−84.
(39) Mamontov, E.; Vlcek, L.; Wesolowski, D. J.; Cummings, P. T.; Wang, W.; Anovitz, L. M.; Rosenqvist, J.; Brown, C. M.; Sakai, V. G. Dynamics and Structure of Hydration Water on Rutile and Cassiterite Nanopowders Studied by Quasielastic Neutron Scattering and Molecular Dynamics Simulations. *J. Phys. Chem. C* **2007**, *111*, 4328−4341.
(40) Ohto, T.; Mishra, A.; Yoshimune, S.; Nakamura, H.; Bonn, M.; Nagata, Y. Influence of Surface Polarity on Water Dynamics at the Water/Rutile TiO_2(110) Interface. *J. Phys.: Condens. Matter* **2014**, *26*, 244102.
(41) Cromer, D. T.; Herrington, K. The Structure of Anatase and Rutile. *J. Am. Chem. Soc.* **1955**, *77*, 4708−4709.
(42) Marchand, R.; Brohan, L.; Tournoux, M. TiO_2(B) a New Form of Titanium Dioxide and the Potassium Octatitanate $K_2Ti_8O_{17}$. *Mater. Res. Bull.* **1980**, *15*, 1129−1133.
(43) Yuet, P. K.; Blankschtein, D. Molecular Dynamics Simulation Study of Water Surfaces: Comparison of Flexible Water Models. *J. Phys. Chem. B* **2010**, *114*, 13786−13795.
(44) Bandura, A. V.; Kubicki, J. D. Derivation of Force Field Parameters for TiO_2-H_2O Systems from Ab Initio Calculations. *J. Phys. Chem. B* **2003**, *107*, 11072−11081.
(45) LAMMPS; http://lammps.sandia.gov.
(46) Hockney, R. W.; Eastwood, J. W. *Computer Simulation Using Particles*, 2nd ed.; IOP: Bristol, U.K., 1988.
(47) Henderson, M. A. The Interaction of Water with Solid Surfaces: Fundamental Aspects Revisited. *Surf. Sci. Rep.* **2002**, *46*, 1−308.
(48) Hodgson, A.; Haq, S. Water Adsorption and the Wetting of Metal Surfaces. *Surf. Sci. Rep.* **2009**, *64*, 381−451.
(49) Chabal, Y. J. Surface Infrared-Spectroscopy. *Surf. Sci. Rep.* **1988**, *8*, 211−357.
(50) Feibelman, P. J.; Kimmel, G. A.; Smith, R. S.; Petrik, N. G.; Zubkov, T.; Kay, B. D. A Unique Vibrational Signature of Rotated Water Monolayers on Pt(111): Predicted and Observed. *J. Chem. Phys.* **2011**, *134*, 204702.
(51) Lindan, P. J. D.; Harrison, N. M.; Holender, J. M.; Gillan, M. J. First-Principles Molecular Dynamics Simulation of Water Dissociation on TiO_2(110). *Chem. Phys. Lett.* **1996**, *261*, 246−252.
(52) Kumar, N.; Neogi, S.; Kent, P. R. C.; Bandura, A. V.; Kubicki, J. D.; Wesolowski, D. J.; Cole, D.; Sofo, J. O. Hydrogen Bonds and Vibrations of Water on (110) Rutile. *J. Phys. Chem. C* **2009**, *113*, 13732−13740.
(53) English, N. J. Dynamical Properties of Physically Adsorbed Water Molecules at the TiO_2 Rutile-(110) Surface. *Chem. Phys. Lett.* **2013**, *583*, 125−130.
(54) Lun Pang, C.; Lindsay, R.; Thornton, G. Chemical Reactions on Rutile TiO_2(110). *Chem. Soc. Rev.* **2008**, *37*, 2328−2353.
(55) Dahal, A.; Dohnálek, Z. Formation of Metastable Water Chains on Anatase TiO_2(101). *J. Phys. Chem. C* **2017**, *121*, 20413−20418.
(56) Brookes, I. M.; Muryn, C. A.; Thornton, G. Imaging Water Dissociation on TiO_2(110). *Phys. Rev. Lett.* **2001**, *87*, 266103.
(57) Tilocca, A.; Selloni, A. Vertical and Lateral Order in Adsorbed Water Layers on Anatase TiO_2(101). *Langmuir* **2004**, *20*, 8379−8384.
(58) Beck, T. J.; Klust, A.; Batzill, M.; Diebold, U.; Di Valentin, C.; Tilocca, A.; Selloni, A. Mixed Dissociated/Molecular Monolayer of Water on the TiO_2(011)-(2 × 1) Surface. *Surf. Sci.* **2005**, *591*, L267−L272.
(59) Di Valentin, C.; Tilocca, A.; Selloni, A.; Beck, T. J.; Klust, A.; Batzill, M.; Losovyj, Y.; Diebold, U. Adsorption of Water on Reconstructed Rutile TiO_2(011)-(2 × 1):Ti = O Double Bonds and Surface Reactivity. *J. Am. Chem. Soc.* **2005**, *127*, 9895−9903.

DOI: 10.1021/acs.jced.7b00984
J. Chem. Eng. Data 2018, 63, 2420−2429

(60) Vittadini, A.; Casarin, M.; Selloni, A. Structure and Stability of TiO_2-B Surfaces: A Density Functional Study. *J. Phys. Chem. C* **2009**, *113*, 18973−18977.
(61) Vittadini, A.; Casarin, M.; Selloni, A. Hydroxylation of TiO_2-B: Insights from Density Functional Calculations. *J. Mater. Chem.* **2010**, *20*, 5871.
(62) Deshmukh, S. A.; Sankaranarayanan, S. K. Atomic Scale Characterization of Interfacial Water near an Oxide Surface using Molecular Dynamics Simulations. *Phys. Chem. Chem. Phys.* **2012**, *14*, 15593−605.
(63) Martí, J.; Padro, J. A.; Guàrdia, E. Molecular Dynamics Simulation of Liquid Water along the Coexistence Curve: Hydrogen Bonds and Vibrational spectra. *J. Chem. Phys.* **1996**, *105*, 639−649.
(64) Yang, Z.; Li, Y.; Zhou, G.; Chen, X.; Tao, D.; Hu, N. Molecular Dynamics Simulations of Hydrogen Bond Dynamics and Far-Infrared Spectra of Hydration Water Molecules around the Mixed Monolayer-Protected Au Nanoparticle. *J. Phys. Chem. C* **2015**, *119*, 1768−1781.
(65) Tay, K.; Bresme, F. Hydrogen Bond Structure and Vibrational Spectrum of Water at a Passivated Metal Nanoparticle. *J. Mater. Chem.* **2006**, *16*, 1956.
(66) Xantheas, S. S.; Dunning, T. H. Ab Initio Studies of Cyclic Water Clusters $(H_2O)n$, n = 1−6. I. Optimal Structures and Vibrational Spectra. *J. Chem. Phys.* **1993**, *99*, 8774−8792.
(67) Fredin, L.; Nelander, B.; Ribbegård, G. Infrared Spectrum of the Water Dimer in Solid Nitrogen. I. Assignment and Force Constant Calculations. *J. Chem. Phys.* **1977**, *66*, 4065−4072.
(68) Levchenko, A. A.; Kolesnikov, A. I.; Ross, N. L.; Woodfield, B. F.; Li, G.; Navrotsky, A.; Boerio-Goates, J. Dynamics of Water Confined on a TiO_2 (Anatase) Surface. *J. Phys. Chem. A* **2007**, *111*, 12584−12588.
(69) Spencer, E. R.; Levchenko, A. A.; Ross, N. L.; Kolesnikov, A. I.; Boerio-Goates, J.; Woodfield, B. F.; Navrotsky, A.; Li, G. Inelastic Neutron Scattering Study of Confined Surface Water on Rutile Nanoparticles. *J. Phys. Chem. A* **2009**, *113*, 2796−2800.
(70) Kavathekar, R. S.; English, N. J.; MacElroy, J. M. D. Study of Translational, Librational and Intra-Molecular Motion of Adsorbed Liquid Water Monolayers at Various TiO_2 Interfaces. *Mol. Phys.* **2011**, *109*, 2645−2654.
(71) Hehre, W. J.; Radom, L.; Schleyer, P. V. R.; Pople, J. A. *Ab Initio Molecular Orbital Theory*; Wiley: New York, 1986.
(72) Alecu, I. M.; Zheng, J. J.; Zhao, Y.; Truhlar, D. G. Computational Thermochemistry: Scale Factor Database and Scale Factors for Vibrational Frequencies Obtained from Electronic Model Chemistries. *J. Chem. Theory Comput.* **2010**, *6*, 2872−2887.
(73) Merrick, J. P.; Moran, D.; Radom, L. An Evaluation of Harmonic Vibrational Frequency Scale Factors. *J. Phys. Chem. A* **2007**, *111*, 11683−11700.
(74) Andersson, M. P.; Uvdal, P. New Scale Factors for Harmonic Vibrational Frequencies Using the B3LYP Density Functional Method with the Triple-ζ Basis Set 6-311+G(d,p). *J. Phys. Chem. A* **2005**, *109*, 2937−2941.
(75) Rauhut, G.; Pulay, P. Transferable Scaling Factors for Density Functional Derived Vibrational Force Fields. *J. Phys. Chem.* **1995**, *99*, 3093−3100.
(76) El-Azhary, A. A.; Suter, H. U. Comparison between Optimized Geometries and Vibrational Frequencies Calculated by the DFT Methods. *J. Phys. Chem.* **1996**, *100*, 15056−15063.
(77) Scott, A. P.; Radom, L. Harmonic Vibrational Frequencies: An Evaluation of Hartree-Fock, Møller-Plesset, Quadratic Configuration Interaction, Density Functional Theory, and Semiempirical Scale Factors. *J. Phys. Chem.* **1996**, *100*, 16502−16513.
(78) Zhou, G. B.; Li, Y. Z.; Yang, Z.; Fu, F. J.; Huang, Y. P.; Wan, Z.; Li, L.; Chen, X. S.; Hu, N.; Huang, L. L. Structural Properties and Vibrational Spectra of Ethylammonium Nitrate Ionic Liquid Confined in Single-Walled Carbon Nanotubes. *J. Phys. Chem. C* **2016**, *120*, 5033−5041.
(79) Byl, O.; Liu, J. C.; Wang, Y.; Yim, W. L.; Johnson, J. K.; Yates, J. T., Jr. Unusual Hydrogen Bonding in Water-Filled Carbon Nanotubes. *J. Am. Chem. Soc.* **2006**, *128*, 12090−12097.
(80) Weinwurm, M.; Dellago, C. Vibrational Spectroscopy of Water in Narrow Nanopores. *J. Phys. Chem. B* **2011**, *115*, 5268−77.
(81) Luzar, A.; Chandler, D. Hydrogen-Bond Kinetics in Liquid Water. *Nature* **1996**, *379*, 55−57.
(82) Stillinger, F. H. Water Revisited. *Science* **1980**, *209*, 451−457.
(83) Zhao, W.; Leroy, F.; Heggen, B.; Zahn, S.; Kirchner, B.; Balasubramanian, S.; Müller-Plathe, F. Are There Stable Ion-Pairs in Room-Temperature Ionic Liquids? Molecular Dynamics Simulations of 1-n-Butyl-3-Methylimidazolium Hexafluorophosphate. *J. Am. Chem. Soc.* **2009**, *131*, 15825−15833.
(84) Karimi-Varzaneh, H. A.; Carbone, P.; Muller-Plathe, F. Hydrogen Bonding and Dynamic Crossover in Polyamide-66: A Molecular Dynamics Simulation Study. *Macromolecules* **2008**, *41*, 7211−7218.

DOI: 10.1021/acs.jced.7b00984
J. Chem. Eng. Data 2018, 63, 2420−2429